Atmos. Chem. Phys., 24, 13285–13297, 2024
https://doi.org/10.5194/acp-24-13285-2024

Atmospheric Chemistry and Physics
Open Access
EGU

Brownness of organics in anthropogenic biomass burning aerosols over South Asia

Chimurkar Navinya[1], Taveen Singh Kapoor[2], Gupta Anurag[1,3], Chandra Venkataraman[1,4], Harish C. Phuleria[1,3], and Rajan K. Chakrabarty[2]

[1]Centre for Climate Studies, Indian Institute of Technology Bombay, Mumbai, 400076, India
[2]Center for Aerosol Science and Engineering, Department of Energy, Environmental and Chemical Engineering, Washington University in St. Louis, St. Louis, MO 63130, USA
[3]Environmental Science and Engineering Department, Indian Institute of Technology Bombay, Mumbai, 400076, India
[4]Department of Chemical Engineering, Indian Institute of Technology Bombay, Mumbai, 400076, India

Correspondence: Chandra Venkataraman (chandra@iitb.ac.in) and Rajan K. Chakrabarty (chakrabarty@wustl.edu)

Received: 2 May 2024 – Discussion started: 23 May 2024
Revised: 9 October 2024 – Accepted: 13 October 2024 – Published: 2 December 2024

Abstract. In South Asia, biomass is burned for energy and waste disposal, producing brown carbon (BrC) aerosols whose climatic impacts are highly uncertain. To assess these impacts, a real-world understanding of BrC's physio-optical properties is essential. For this region, the order-of-magnitude variability in BrC's spectral refractive index as a function of particle volatility distribution is poorly understood. This leads to oversimplified model parameterization and subsequent uncertainty in regional radiative forcing. Here we used the field-collected aerosol samples from major anthropogenic biomass activities to examine the methanol-soluble BrC optical properties. We show a strong relation between the absorption strength, wavelength dependence, and thermo-optical fractions of carbonaceous aerosols. Our observations show strongly absorbing BrC near the Himalayan foothills that may accelerate glacier melt, further highlighting the limitations of climate models where variable BrC properties are not considered. These findings provide crucial inputs for refining climate models and developing effective regional strategies to mitigate BrC emissions.

1 Introduction

Carbonaceous aerosols, such as black and organic carbon, make up most fine particulate matter ($PM_{2.5}$) emissions globally (McDuffie et al., 2020; Roy et al., 2023; Kurokawa and Ohara, 2020; Crippa et al., 2018) and ∼ 40 % over South Asia (Tibrewal et al., 2024; Pandey et al., 2014; Sadavarte et al., 2019). Anthropogenic biomass usage for residential cooking and heating (Pandey et al., 2014; Habib et al., 2023; Navinya et al., 2023), residue burning for agricultural waste disposal (Kapoor et al., 2023b; Azhar et al., 2019), and biomass-fired brick kilns (Weyant et al., 2014; Tibrewal et al., 2023) are the common sources of these carbonaceous aerosols across South Asia (Tibrewal et al., 2024; Pandey et al., 2014; Sadavarte et al., 2019; Ohara et al., 2007) and many other developing countries (Bonjour et al., 2013; Yevich and Logan, 2003; McDuffie et al., 2020). These aerosols perturb the Earth's energy balance, depending on their mixing state, size distribution, wavelength dependence of optical properties, and absorption strength (Zhang et al., 2020; Neyestani and Saleh, 2022; Brown et al., 2018; Arola et al., 2015; Bond and Bergstrom, 2006). However, the extent of this perturbation remains uncertain (Szopa et al., 2021; Gliß et al., 2021). Over the last 2 decades, extensive research has focused on the climate impact of highly absorbing black carbon (BC) (Bond et al., 2013). In contrast, the climate implications of light-absorbing organic carbon (OC), termed brown carbon (BrC), have received relatively little attention and are thus less cer-

tain (Saleh et al., 2018; Brown et al., 2018; Saleh, 2020). The chemical composition of BrC varies significantly, and consequently its optical properties, as reported across previous studies, span orders of magnitude in the imaginary refractive index (k) values that determine its light-absorbing strength (Chakrabarty et al., 2023; Choudhary et al., 2021, 2018, 2017; Dey et al., 2021; Kapoor et al., 2023a; Kirillova et al., 2016; Rana et al., 2020; Rathod et al., 2017; Saleh et al., 2018, 2014; Srinivas and Sarin, 2014). Previous studies have often measured aged ambient BrC that is weakly absorbing ($k_{\mathrm{BrC},550} < 0.01$) due to photobleaching (Sumlin et al., 2017); hence some climate impact assessment studies have regarded BrC as a weakly absorbing or non-absorbing particle (Lee et al., 2010; Sand et al., 2021; Zhang et al., 2020). However, this underestimates the impact of freshly emitted BrC that has high absorption strength ($k_{\mathrm{BrC},550} > 0.1$) and resists photobleaching, resulting in an extended atmospheric lifetime (Chakrabarty et al., 2023). Furthermore, the formation of light-absorbing secondary BrC and the enhancement of BC absorption due to OC coating (Rastogi et al., 2021; Bhowmik et al., 2024; Kapoor et al., 2022) add complexity to radiative transfer models.

BrC has a wide range of absorption strengths; studies show $k_{\mathrm{BrC},550}$ varying from ~ 0.007 (Islam et al., 2022) to ~ 0.2 (Chakrabarty et al., 2023). In addition to the different methods used to derive BrC optical information, such variation is associated with the different combustion conditions (Saleh et al., 2018), aging of BrC (Sumlin et al., 2017; Dasari et al., 2019; Romonosky et al., 2016; Chen et al., 2021), and secondary reactions (Wang et al., 2020; Kroll et al., 2007; Kroll and Seinfeld, 2008; Hecobian et al., 2010). An experimental study explained that the progressive transformation of BC precursors to BC results from different combustion conditions, which create the BrC–BC light absorption continuum (Saleh et al., 2018). This continuum shows an increase in the absorption strength of carbonaceous aerosols that is associated with a decrease in wavelength dependence (w), solubility, and volatility (Saleh, 2020). Recent studies have also observed such a relationship but for a smaller range of k_{BrC} values (< 0.01) (Devaprasad et al., 2024; Luo et al., 2022). However, information about real-world source-specific BrC absorption and its position in the BrC–BC continuum is lacking. Understanding this light absorption continuum alongside carbonaceous aerosol emissions aids BrC parameterization in climate models (Zhang et al., 2020; Saleh et al., 2014). Presently, because source-specific BrC information is absent from emission inventories, many climate models inadequately account for BrC. Studies have used the BrC-to-BC ratio along with k_{BrC} to understand its direct radiative effect (Park et al., 2010; Feng et al., 2013). Furthermore, other studies (Zhang et al., 2020; Neyestani and Saleh, 2022; Brown et al., 2018) have employed BrC parameterization schemes based on laboratory-generated data to address the climate impact of BrC, but this approach might not adequately represent real-world biomass burning conditions (Saleh et al., 2014; Lu et al., 2015). Hence, regions with high OC emissions and stronger BrC (S-BrC), also known as dark BrC ($k_{\mathrm{BrC},550} > 0.1$), could have a high climate impact caused by persistent BrC, which is possibly underestimated in the absence of regional source-specific BrC data.

The recent Carbonaceous Aerosol Emissions, Source Apportionment and Climate Impacts (COALESCE) field emission measurement campaigns and questionnaire surveys in India (Navinya et al., 2023; Kapoor et al., 2023b; Tibrewal et al., 2023; Habib et al., 2023) have prepared a comprehensive inventory encompassing both formal (transportation, industries, and power generation) and informal (residential, agricultural residue burning, and brick production) emission sectors (Venkataraman et al., 2020; Tibrewal et al., 2024). The emission estimates show the substantial contribution of anthropogenic $PM_{2.5}$ in India from biomass fuel burning practices for residential cooking and agricultural residue burning (Kapoor et al., 2023b; Tibrewal et al., 2024; Habib et al., 2023). Recent studies have highlighted considerable biomass consumption for residential heating and brick production (Tibrewal et al., 2023; Navinya et al., 2023). Figure 1 shows that 91 % of the OC emissions ($3\,\mathrm{Tg\,yr^{-1}}$) over India are from three sources: residential cooking (COOK), heating (HEAT), and agricultural residue burning (AGRI), with most emissions from the Indo-Gangetic Plain ($\sim 50\,\%$) (Tibrewal et al., 2024). The unexplored climate impacts of OC emitted from these biomass-based sources make the Indian subcontinent particularly prone to environmental challenges.

This study leverages samples of aerosol particle emissions collected on filter substrates during the COALESCE field campaign to evaluate BrC–BC light absorption continuum behavior in real-world biomass burning emissions. Using a UV–Vis spectrophotometer, we examine BrC derived from major biomass fuel sources such as cooking, heating, agricultural residue burning, and brick production. The study aims to connect BrC with the thermo-optically resolved carbon fractions to parameterize BrC absorption over South Asia. Further, it endeavors to couple source-specific BrC properties with the BC-to-organic aerosol (OA) ratio to explore the spatial variability in the absorption properties of BrC emitted across India.

2 Data and methods

2.1 Data collection

A field-based emission measurement campaign (Fig. S2 in the Supplement) was conducted from October 2021 to April 2022 in rural parts of Gujarat and Maharashtra, two western Indian states. These locations were selected based on their representativeness of the fuels and devices commonly used in South Asia based on previous studies (Navinya et al., 2023; Kapoor et al., 2023b; Tibrewal et al., 2023; Habib et al., 2023). The primary aim of this campaign was to capture physical, chemical, and optical information about the

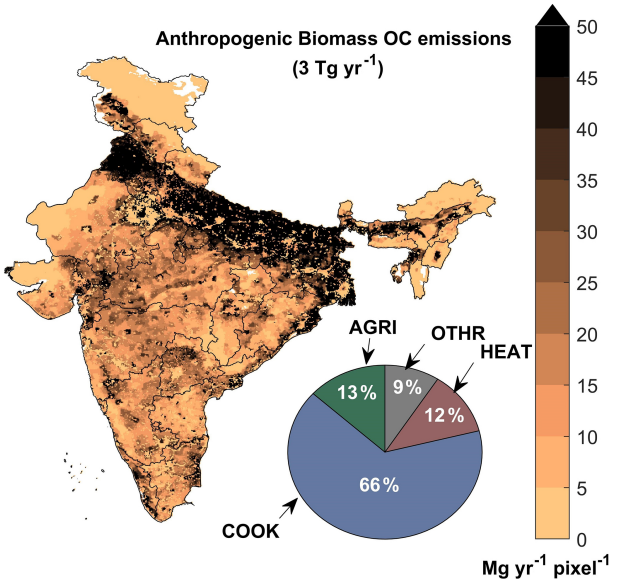

Figure 1. The spatial distribution of OC emissions ($Mg\,yr^{-1}$ per pixel) from three major sources – agricultural residue burning (AGRI), residential cooking (COOK), and residential heating (HEAT) – covers ∼ 91 % of the total OC emissions ($3.3\,Tg\,yr^{-1}$) over India. OC emissions are taken from the Carbonaceous Aerosol Emissions, Source Apportionment and Climate Impacts (COALESCE) Speciated Multipollutant Generator for India (SMoG-India) emission inventory for the year 2019 (Tibrewal et al., 2024). Here, the pixel size is 5 km × 5 km. The pie chart represents the shares of anthropogenic biomass burning sources in the total OC emissions over India. Other sources (OTHR) of OC include brick production, transportation, industries, and power generation. Publisher's remark: please note that the above figure contains disputed territories.

emissions from biomass sources: agricultural residue burning, brick production from clamps, cooking, and heating. The source emission sampling system, as described by Kumari et al. (2024) and Venkataraman et al. (2020), consists of a multi-arm inlet design adapted from Roden et al. (2006) to function as an area plume sampler, positioned 1 to 1.5 m above the emission source (Fig. S2). The system comprises eight arms that aspirate aerosols, which are then combined in a mixing plenum to ensure representative sampling of the smoke plume. Aerosols drawn through the inlet pass through a 2.5 µm cutoff cyclone and are subsequently divided into two streams for real-time and for time-integrated filter-based measurements. Aerosols from the latter airstream were collected on quartz filter substrates for offline laboratory analysis over the entire duration of the experiment, encompassing the ignition, flaming, and smoldering phases, in order to obtain a sample representative of the complete combustion cycle. The temperatures of the emitted plumes were diluted by the surrounding air, reaching levels close to the temperature of ambient air before entering the multi-arm sampler. This ensured that the emissions had undergone gas-to-particle partitioning, corresponding to the properties of emissions used in climate models. In this study, we utilized aerosol-laden quartz filter substrates from 14 different fuel and source combinations (Table S1 in the Supplement) to understand soluble BrC absorption ($Mm^{-1} = 10^6\,m^{-1}$) and total OC concentration ($\mu g\,m^{-3}$).

2.2 Estimation of BrC properties

We used 4.5 mL of methanol solvent and dissolved two 0.25 in. diameter punches of quartz filters in the solvent. After 1 h of sonication, the extracted solvent was passed through a 0.22 µm polytetrafluoroethylene membrane syringe filter (Fisherbrand™) to remove insoluble debris. The absorption of this methanol-soluble OC (considered BrC absorption) was estimated using a UV–Vis spectrophotometer (LAMBDA 35, PerkinElmer) with a working range of 300 to 900 nm and a spectral resolution of 1 nm. Equation (1) was used to estimate the absorption coefficient at any given wavelength (Chakrabarty et al., 2023; Sarkar et al., 2019; Satish and Rastogi, 2019; Srinivas and Sarin, 2013, 2014; Bikkina et al., 2020; Boreddy et al., 2021; Choudhary et al., 2017, 2018, 2021, 2022; Dasari et al., 2019; Dey et al., 2021; Kirillova et al., 2016; Mukherjee et al., 2020; Rajeev et al., 2022; Rastogi et al., 2021; Rathod et al., 2017; Rana et al., 2020; Shamjad et al., 2016, 2018).

$$b_{\mathrm{abs,BrC},\lambda} = \frac{(A_\lambda - A_{700}) \times V_{\mathrm{Extract}} \times \ln(10)}{V_{\mathrm{Sampled}} \times L \times f_{\mathrm{filter\ area}}} \quad (1)$$

In Eq. (1), A_λ is absorbance at wavelength λ, V_{Extract} is the volume of solvent extract used (4.5 mL in this study), V_{Sampled} is the volume of air sampled, $f_{\mathrm{filter\ area}}$ is the fraction of filter area used for the analysis, and L is the optical path length (0.01 m). Given that soluble BrC does not absorb at wavelengths of 700 nm and longer or, at best, absorbs very little, the absorption at 700 nm (A_{700}) was used to normalize absorbance to account for signal drift within the instrument, which is a limitation of this method. In this study, the estimated BrC only includes the methanol-soluble component and may not fully represent total BrC, including its insoluble components. The estimated BrC absorption could be underestimated due to excluded insoluble BrC and tarball structures, which possess high absorption strength (Corbin et al., 2019; Chakrabarty et al., 2023, 2010). The underestimation may be more pronounced as particle light absorption strength increases, i.e., closer to the dark-BrC region, since particle solubility is inversely proportional to light absorption strength (Saleh, 2020). In brief, Saleh (2020, and references therein) reviewed and categorized different BrC classes based on their volatility, using UV–Vis spectrometry, optical closure (Aethalometer, cavity ring-down spectroscopy, and photoacoustic spectroscopy), and electron energy loss spectroscopy techniques. While UV–Vis spectrometry misses out insoluble particles, optical closure techniques consider absorption by particles regardless of their solubility. However,

they have uncertainties associated with separating BrC light absorption from the total aerosol light absorption. In this study only two data points, observed marginally in the dark-BrC region, might be affected.

Quartz filters were examined using a Magee Scientific DRI multi-wavelength thermo-optical carbon analyzer with the IMPROVE_A protocol to estimate the elemental carbon (EC) and organic carbon (OC) concentrations (Chow et al., 2007). Thermo-optically resolved carbon fractions (OC1, OC2, OC3, OC4, EC1, EC2, and EC3) were used after pyrolytic correction to reconstruct the total organic carbon and total elemental carbon fractions (Chow et al., 2007). For the purpose of representation in Fig. 3, pyrolytic carbon was assigned to OC4. These fractions are associated with the volatility of the OC (Kapoor et al., 2023a; Shetty et al., 2023; Tohidi et al., 2022; Vodička et al., 2015; Soleimanian et al., 2019; Ma et al., 2016), as these OC fractions are measured under increasing temperature peaks (140, 280, 480, and 580 °C) during thermo-optical analysis. Hence, OC1 exhibits relatively high volatility compared to OC2, while OC2 is more volatile than OC3, and similarly, OC3 shows more volatility than OC4. In this study, pyrolysis-corrected EC was treated as a proxy for BC to facilitate the comparison with other studies. The uncertainties associated with OC and EC measurements are 5 % and 10 %, respectively (Cheng et al., 2021; DRI Manual, 2015). Cheng et al. (2021) reported an overall uncertainty of approximately 10 % for methanol-soluble k_{BrC} determined through UV–Vis spectrophotometry. When accounting for the 5 % manufacturer-reported uncertainty in OC concentration, the corresponding uncertainty in the absorption coefficient is estimated to be around 10 %.

Furthermore, OC concentration and $b_{\mathrm{abs,BrC},\lambda}$ were used to calculate the mass absorption coefficient ($\mathrm{MAC}_{\mathrm{BrC},\lambda}$). The imaginary refractive index of BrC ($k_{\mathrm{BrC},\lambda}$) was estimated by considering the density (ρ) of freshly emitted OC to be 1500 kg m^{-3} (Liu et al., 2013; Shamjad et al., 2016), using the following relation (Jennings et al., 1979):

$$k_{\lambda} = \frac{\rho \times \lambda \times \mathrm{MAC}_{\lambda}}{4\pi}. \quad (2)$$

The same equation has been used in many previous studies, some of which cover the same geographic region (Shamjad et al., 2018; Bikkina and Sarin, 2019; Shamjad et al., 2016; Rana et al., 2020; Liu et al., 2013; Zhang et al., 2020). In addition, an absorption Ångström exponent (AAE) between 365 and 550 nm ($\mathrm{AAE}_{365/550} = -\ln(b_{\mathrm{abs,BrC},365}/b_{\mathrm{abs,BrC},550})/\ln(365/550)$) was also estimated to understand the spectral dependence of the BrC absorption coefficient. Similarly, w (AAE-1) indicates the spectral dependence of the imaginary refractive index between 365 nm (a commonly used wavelength for studying BrC absorption) and 550 nm (the peak of solar radiation intensity). In this study, we have used w and k for ease of comparison with previous studies (Saleh et al., 2014; Lu et al., 2015; Luo et al., 2022; Saleh et al., 2018). However, AAE and MAC can also be used alternatively.

2.3 Spatial variation in BrC absorption

The relationship between fuel- and source-averaged $k_{\mathrm{BrC},550}$ and the BC-to-OA ratio ($k_{\mathrm{BrC},550} = 0.0365(\pm 0.006) \times (\mathrm{BC/OA}) + 0.0047(\pm 0.0037)$, $R^2 = 0.93$) was established using field-collected fuel samples. Similarly, w was also calculated as a function of the BC-to-OA ratio ($w = 5.355(\pm 0.50) \times \exp(-0.428(\pm 0.25) \times (\mathrm{BC/OA})$; $R^2 = 0.60$). Here, OA was derived by multiplying OC by a factor of 1.8, a methodology consistent with previous studies (Turpin and Lim, 2001; Chow et al., 2015; Navinya et al., 2020; Provençal et al., 2017; Kumar et al., 2023) and aligned with the OA density considered (Kuwata et al., 2012). Although this factor does not impact the R squared (R^2) of the relationship, it facilitates comparisons with other studies that have utilized the BC-to-OA ratio to derive $k_{\mathrm{BrC},550}$. The spatial distribution of BC and OC emissions from the SMoG-India emission inventory (Tibrewal et al., 2024) was integrated into the equation, after converting OC into OA using the same factor, to calculate the nationwide $k_{\mathrm{BrC},550}$ and w for the major (∼ 90 %) OC-emitting sources: AGRI, COOK, and HEAT. Additionally, we derived overall k_{BrC} and w values through a weighted averaging approach, incorporating OC emissions (Fig. S5 in the Supplement) as weights along with source-specific information (Fig. S3 in the Supplement). BRICK (brick production) was omitted because field-based samples were limited to clamp kilns and not available for other major brick production technologies, including Bull's trench kilns and vertical shaft brick kilns (Weyant et al., 2014; Tibrewal et al., 2024, 2023).

3 Results and discussion

3.1 BrC–BC absorption continuum

The measured $k_{\mathrm{BrC},550}$ values varied from 0.0007 to 0.1199, while w ranged from 7.52 to 1.00, highlighting the inverse dependence of k_{BrC} on w (Fig. 2). A previous study using synthetic fuels under different combustion conditions reported a similar observation based on experimental measurements (Saleh et al., 2018). Relative to the present study, different field-collected sources and fuels reflected real-world variations in burning practices. An equation fitted to the data ($w = 0.1917/(k_{\mathrm{BrC},550} + 0.02886)$) has an R^2 value of 0.58, and an extension of this curve with 95 % prediction bounds overlaps the BC absorption region ($k_{550} = 0.6$–0.8 and $w = \sim 0$–0.2) (Bond and Bergstrom, 2006; Saleh et al., 2018; Liu et al., 2018; Gyawali et al., 2013). The range of $k_{\mathrm{BrC},550}$ and w values observed in this study spans three broad classes of BrC (weak, moderate, and strong) suggested by Saleh (2020) for different combustion conditions. Saleh (2020) suggests that while combustion processes emit

particles containing a mix of different BrC classes, smoldering biomass emissions are skewed more toward weakly absorbing BrC (W-BrC), while high-temperature biomass combustion emissions are skewed more toward moderately and strongly absorbing BrC (M-BrC and S-BrC). In the present work, some data points, mainly from cooking and heating, exhibit greater spectral variation (larger w) than that suggested for M-BrC, while falling within its $k_{BrC,550}$ range. Changing combustion conditions were observed during several experiments, where both flaming and smoldering combustion phases occurred, while particles were collected as a time-averaged filter sample. Here, the greater spectral dependence in M-BrC measurements implies that these samples would exert stronger light absorption in the near-UV range than typical M-BrC would. The thermo-optically resolved carbon fractions show a decline in the total OC fraction, mainly in OC1 and OC2 (relatively high volatility fractions), with increasing BrC absorption strength from weak to moderate (Fig. 3a). A simultaneous increase in EC highlights the dominance of BC absorption as the strength of BrC absorption increases, as also reported previously (Saleh et al., 2014; Chakrabarty et al., 2023). Relationships between BC, OC, and BrC properties, reported by Saleh et al. (2014), are useful in parameterizing BrC absorption in radiative and climate models (Brown et al., 2018; Neyestani and Saleh, 2022; Wang et al., 2018).

3.2 Source-specific BrC

We observed that the variability in source-specific BrC properties is larger within a source category than among different source categories. Figure 3b shows no significant changes in $k_{BrC,550}$ among different source categories. However, there are much larger differences among individual data points in a source category because of varying fuels, meteorology, and burning practices. The $k_{BrC,550}$ means from agricultural residue burning, brick production, cooking, and heating are 0.026 ($\pm$0.035), 0.015 ($\pm$0.026), 0.015 ($\pm$0.003), and 0.010 ($\pm$0.006), respectively (Fig. 3b). A large variation in $k_{BrC,550}$ was observed during agricultural residue burning, with banana, which has a high moisture content (Tock et al., 2010) showing a $k_{BrC,550}$ of 0.008, and pigeon pea (an oilseed legume), which has a $k_{BrC,550}$ of 0.082. In comparison, $k_{BrC,550}$ varies from 0.006 (final stage) to 0.022 (initial stage) during brick kiln operation and from 0.002 (crop residue) to 0.013 (firewood) during residential heating. This contrasts with cooking, where deliberate efforts are made to ensure efficient burning of fuel for meal preparation. Hence, BrC properties in cooking emissions do not vary much ($k_{BrC,550} = 0.015 \pm 0.001$). Our study observed $k_{BrC,365}$ of $\sim$0.1 ($\pm$0.01) for cooking, which is higher than lab-measured values (0.014–0.054) for the same fuels at 350 nm (Rathod et al., 2017). We observed that $MAC_{BrC,365}$ stayed between 1.5–2.5 $m^2\,g^{-1}$ for all source–fuel combinations, except for pigeon pea residue burning ($MAC_{BrC,365} = 4.01\ m^2\,g^{-1}$). The current findings are comparable with the $MAC_{BrC,365}$ value of 2 ($\pm$0.5) $m^2\,g^{-1}$ from Indian air masses influenced by agricultural residue burning (Satish et al., 2020). The values reported in our study are in the upper range of ambient $MAC_{BrC,365}$ (0.62–2.3 $m^2\,g^{-1}$) reported previously over India (Sarkar et al., 2019; Shamjad et al., 2018; Satish et al., 2020; Rastogi et al., 2021; Rana et al., 2020; Kirillova et al., 2016; Dey et al., 2021), which could be due to photobleaching of ambient BrC that decreases MAC. However, our estimation of $MAC_{BrC,365}$ aligns well with the previously reported source-specific values (1.09–2.53) (Pandey et al., 2020; Debbarma et al., 2024; Rathod et al., 2017). The observed AAE_{BrC} ($\sim 5.23 \pm 1.51$, range 2–8.5; see Table S1) is comparable with previous observations ($\sim 5.31 \pm 1.67$, range 2.3–6.8) for biomass burning over India (Islam et al., 2022; Pandey et al., 2020; Rathod et al., 2017; Satish et al., 2020). In agricultural residue burning, banana residue shows the lowest $k_{BrC,550}$ (0.008) and BC-to-OA ratio (0.030) (Table 2 in the Supplement). In contrast, pigeon pea residue burning has the highest $k_{BrC,550}$ (0.082) and BC-to-OA ratio (2.054). A similar relationship between $k_{BrC,550}$ and BC-to-OA ratio has also been observed in other source–fuel combinations and has been used to parameterize $k_{BrC,550}$ and w (Fig. 4).

3.3 Parameterization of k_{BrC} and w

We leveraged the significant correlation (p value < 0.01) between the BC-to-OA ratio and the BrC properties ($k_{BrC,550}$, $R^2 = 0.93$; w, $R^2 = 0.60$) to build a relationship between these quantities. Despite the variety of fuel burning technologies used, such as traditional stoves, open residue burning, and brick clamps, $k_{BrC,550}$ variability is explained ($R^2 = 0.93$) by the BC-to-OA ratio. We observed that $k_{BrC,550}$ varies linearly from 0.006 to 0.74 for BC-to-OA ratios of 0 to 20 (Fig. 4a). Similarly, we explain w using the BC-to-OA ratio to provide an approximation of the BrC absorption over the different wavelengths. We observed an exponential relation between w and the BC-to-OA ratio with an R^2 of 0.60 (w varies from 5 to $\sim$0 for BC-to-OA ratios of 0 to 20, respectively) (Fig. 4b). Relatively to the present studies, the relationship used in climate modeling studies (Zhang et al., 2020; Neyestani and Saleh, 2022; Brown et al., 2018) given by Saleh et al. (2014) would overestimate the $k_{BrC,550}$ over South Asia (Fig. S7 in the Supplement). In contrast, previous studies (Saleh et al., 2014; Lu et al., 2015; Luo et al., 2022) underestimate the range of w values observed in this study, which may result in an underestimation of $k_{BrC,365}$ (Fig. S7). Such an underestimation would propagate uncertainties to radiative forcing calculations, especially over South Asia.

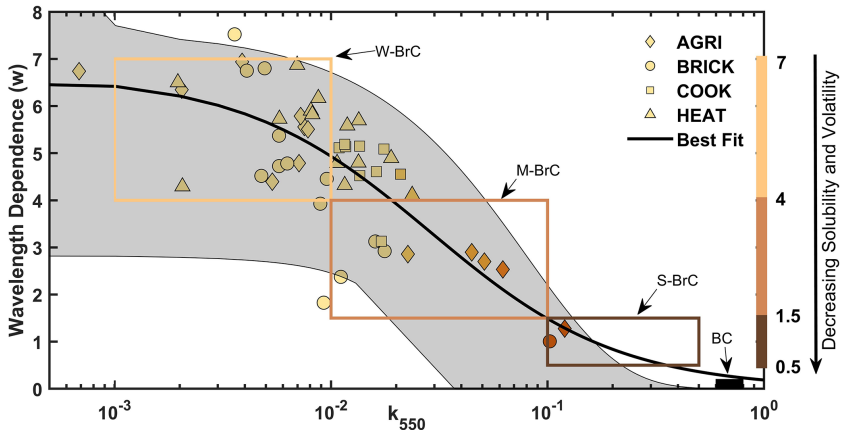

Figure 2. BrC–BC light absorption continuum on a semi-log scale, showing the wavelength dependence ($w = \text{AAE-1}$) of the imaginary part of the refractive index (k_{550}) versus the imaginary part of the refractive index at 550 nm (k_{550}), $w = 0.1917(\pm 0.074)/(k_{\text{BrC},550} + 0.02886(\pm 0.014))$. Here, the BC region lies between $k_{550} = 0.6$–0.8 and $w = 0$–0.2. The BrC classes are defined per Saleh (2020): strongly absorbing BrC (S-BrC), moderately absorbing BrC (M-BrC), and weakly absorbing BrC (W-BrC). The arrow at the right indicates the reduction in the solubility and volatility with an increase in k_{550} (Saleh, 2020). The shaded grey area represents the continuum reported by previous studies (Saleh et al., 2014; Lu et al., 2015; Luo et al., 2022; Saleh et al., 2018), and the equations for the shaded area are given in Sect. S1 and Fig. S1 in the Supplement. The right axis displays the range of wavelength dependencies for the three BrC classes.

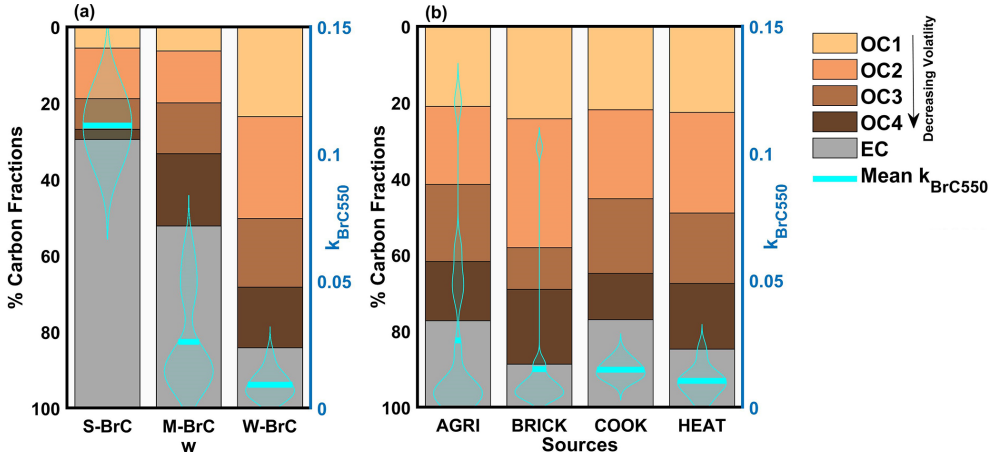

Figure 3. **(a)** $k_{\text{BrC},550}$ distribution (right) and thermo-optically resolved carbon fractions (left) with varying BrC classes based on wavelength dependence. Here, the strongly absorbing BrC (S-BrC), moderately absorbing BrC (M-BrC), and weakly absorbing BrC (W-BrC) ranges are < 1.5, 1.5–4, and > 4, respectively, in terms of wavelength dependence (Saleh, 2020). **(b)** Source-specific $k_{\text{BrC},550}$ distribution (right) and thermo-optically resolved carbon fractions (left). The distributions of violin plots show the kernel density. The arrow near the legend indicates the reduction in the relative volatility from OC1 to OC4 (Ma et al., 2016). For the purpose of representation, pyrolytic carbon was assigned to OC4.

3.4 Spatial differences in $k_{\text{BrC},365}$ and w

Several studies have reported ambient BrC absorption in the South Asian region (Dey et al., 2023; Srinivas and Sarin, 2013, 2014; Bikkina et al., 2020; Boreddy et al., 2021; Choudhary et al., 2017, 2018, 2022; Dasari et al., 2019; Dey et al., 2021; Kirillova et al., 2016; Mukherjee et al., 2020; Rajeev et al., 2022; Rastogi et al., 2021; Rana et al., 2020; Shamjad et al., 2016, 2018), while most climate models continue to consider weakly absorbing BrC absorption (Sand et al., 2021; Feng et al., 2013), regardless of sources and combustion conditions. Feng et al. (2013) simulated global BrC absorption using k_{BrC} values that are 2- to 5-fold weaker than those observed in our study, and they noted underestimation of BrC absorption efficiency over South Asia owing to the presence of strongly absorbing BrC. Other studies (Brown et al., 2018; Zhang et al., 2020) have used $k_{\text{BrC},550}$ values (Saleh et al., 2014; Mcmeeking, 2008) that are 2- to 3-fold higher than those observed in this study to simulate the global radiative impact of BrC. Hence, neglecting the spatial variability in k_{BrC} could lead to bias in under-

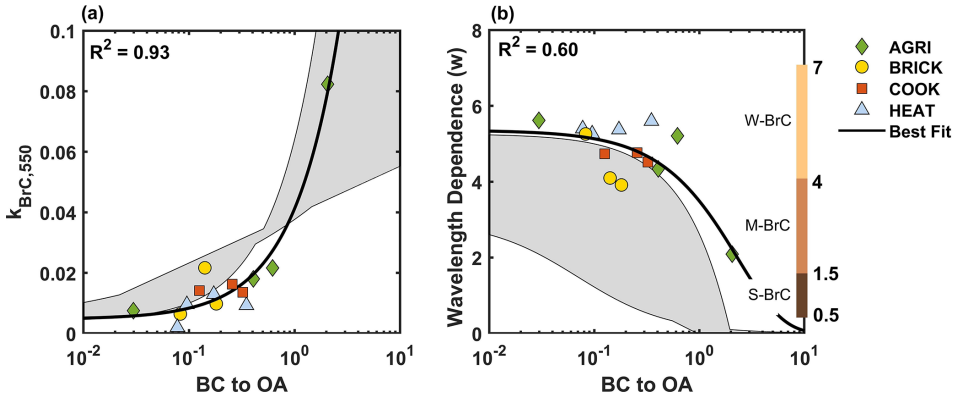

Figure 4. **(a)** Mean $K_{\mathrm{BrC},550}$ versus the BC-to-OA ratio ($k_{\mathrm{BrC},550} = 0.0365(\pm 0.006) \times (\mathrm{BC/OA}) + 0.0047(\pm 0.0037)$; $R^2 = 0.93$) and **(b)** w versus the BC-to-OA ratio ($w = 5.355(\pm 0.50) \times \exp(-0.428(\pm 0.25) \times (\mathrm{BC/OA}))$; $R^2 = 0.60$). Here, OA = OC × 1.8: the factor 1.8 is widely used to convert OC into OA (Turpin and Lim, 2001; Chow et al., 2015; Navinya et al., 2020; Provençal et al., 2017; Kumar et al., 2023). The shaded grey area represents the relationship reported by previous studies (Saleh et al., 2014; Lu et al., 2015; Luo et al., 2022), and the equations for the shaded area are given in Sects. S2 and S3 and Fig. S1). The right axis in **(b)** displays the ranges of wavelength dependencies for the three BrC classes.

standing its radiative impact. Thus, we calculated emission-weighted BrC optical properties across the Indian region to demonstrate their spatial heterogeneity in this region. The relationships shown in Fig. 4 were used to make a spatial map of $k_{\mathrm{BrC},550}$, $k_{\mathrm{BrC},365}$, and w, with emission strength from the COALESCE SMoG-India emission inventory (Tibrewal et al., 2024). SMoG-India is a multi-sectoral, multi-pollutant data set available at a 5 km grid resolution, developed under the COALESCE network (Venkataraman et al., 2020), which also facilitated the collection of samples used in the present study.

Figure 1 shows the large OC emissions over the Indo-Gangetic Plain, with annual emissions ranging from 50–70 $\mathrm{Mg\,yr^{-1}}$ per pixel (pixel size is 5 km × 5 km), while other regions emit ∼ 10–20 $\mathrm{Mg\,yr^{-1}}$ per pixel. Emission-weighted spatial information about w (range 4.3–5.3) and $k_{\mathrm{BrC},550}$ (0.006–0.023) aids in the estimation of $k_{\mathrm{BrC},365}$. Figure 5a shows $k_{\mathrm{BrC},365}$ ranges from 0.05 to 0.14, indicating strong absorption in the UV–Vis wavelengths. The Himalayan foothills show large k_{BrC} values compared to other parts of India, mainly due to high BC-to-OA emissions from the predominant heating activity. A recent study highlighted the low photobleaching rate of BrC near Himalayan regions due to the low ambient temperatures (Choudhary et al., 2022). The coincidence of dark-BrC particle emissions in this study, along with their reported extended lifetimes, could result in snow darkening upon deposition along with accelerated snowmelt and glacier melt (Chelluboyina et al., 2024). The northwestern region of India exhibits the highest OC emissions from agricultural residue burning (Fig. S5), primarily from straw residue burning (Kapoor et al., 2023b), which has a relatively low BC-to-OA ratio. Consequently, the k_{BrC} remains lower compared to its values in other regions, such as Maharashtra and Andhra Pradesh, where oilseed crop burning is prevalent (Kapoor et al., 2023b), resulting in a higher BC-to-OA ratio and higher k_{BrC} values. Heating activities are particularly intense in the colder areas, especially in the Himalayan foothills, with higher use of firewood in the eastern India (Navinya et al., 2023), leading to significantly higher BC-to-OA ratios and elevated k_{BrC} in the northern and eastern regions (Fig. S3). In the central Indo-Gangetic Plain, particularly in Uttar Pradesh and Bihar, dung cake is more commonly used for heating (Navinya et al., 2023), which contributes to very low k_{BrC} values. The variation in the BC-to-OA ratio across India due to cooking activities is minimal (0.075–0.125) compared to that from agricultural residue burning (0.025–0.2) and heating (0.025–0.25), resulting in substantially low spatial variation in $k_{\mathrm{BrC},365}$ (0.06–0.08) from cooking (Fig. S3). The $k_{\mathrm{BrC},550}$ values of combustion aerosol emissions from India vary from 0.006 to 0.023 (Fig. S6 in the Supplement), with some hotspots scattered across the country. These numbers highlight the order-of-magnitude increase in $k_{\mathrm{BrC},365}$ compared to $k_{\mathrm{BrC},550}$, with higher values over eastern and northern India. An earlier investigation also noted elevated modeled BrC absorption in the eastern regions of India (Zhu et al., 2021). The substantial emissions of BrC across the country, coupled with the high k_{BrC} values observed in certain other regions, suggest that BrC particles may have significant radiative impacts over the region.

4 Implications

The variability in $k_{\mathrm{BrC,near\text{-}UV}}$ across modeling studies, ranging from 0.045 (Zhang et al., 2020) to 0.168 (Lin et al., 2014), arises from methodological, fuel, and burning condition disparities in the studies reporting BrC absorption properties from lab-based biomass combustion (Kirchstet-

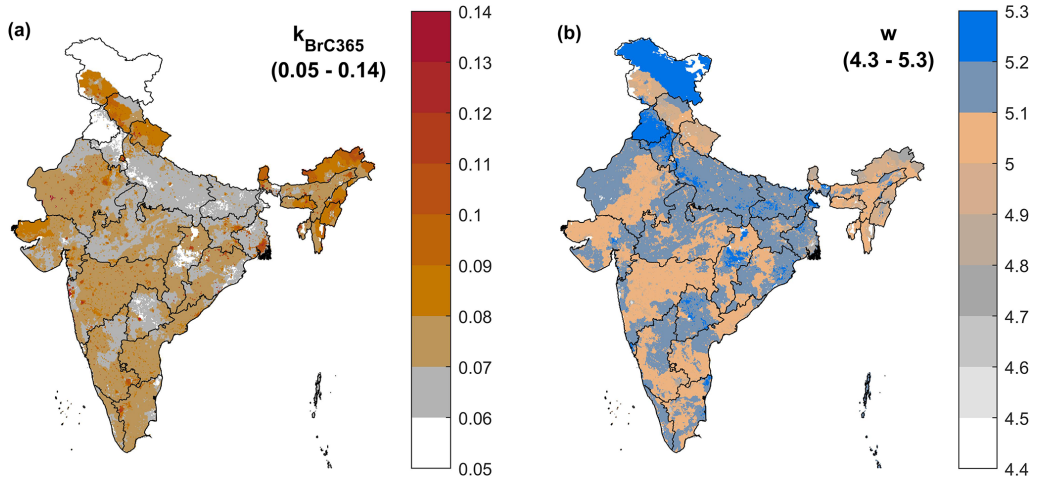

Figure 5. The spatial distribution of **(a)** $k_{BrC,365}$ and **(b)** wavelength dependence (w). The BC-to-OA ratio is taken for the year 2019 from the COALESCE SMoG-India emission inventory (Tibrewal et al., 2024). Publisher's remark: please note that the above figure contains disputed territories.

ter et al., 2004; Chen and Bond, 2010; Lack et al., 2012). However, our study, using field measurements of a variety of sources, introduces source- and fuel-specific k_{BrC} values, enhancing modeling capabilities for a more nuanced understanding of the radiative and climate impacts of BrC. Additionally, the observed varying wavelength dependence (w), linked with the BC-to-OA ratio in this research, amplifies uncertainty when it is assumed to be constant in models (Zhang et al., 2020). Compared to the findings of this study, typical BrC parameterization schemes (Saleh et al., 2014; Lu et al., 2015; Luo et al., 2022) in climate models tend to overestimate $k_{BrC,550}$ while substantially underestimating wavelength dependence, which may misrepresent near-UV BrC absorption in world regions with biomass combustion emissions resembling those in South Asia. Additionally, this study's findings aid in pinpointing biomass fuels and activities, including burning of some agricultural residues and residential space heating, that are both prone to emitting more strongly absorbing BrC ($k_{BrC,550} > 0.1$) and prevalent across developing nations. These variations in k_{BrC} with sources and fuels lead to spatial variations in emitted BrC properties. In the Himalayan foothills, residential space heating produces more strongly absorbing (and more persistent) BrC emissions, and the deposition of these emissions increases the potential risks of increased snow darkening and accelerated glacier melting. Leveraging this information with emission inventories enables the identification and potential interventional targeting of these biomass fuels and activities, with the goal of reducing both their local health impacts and their global climate impacts.

Data availability. The data used in this study are provided in the Supplement of the article.

Supplement. The supplement related to this article is available online at: https://doi.org/10.5194/acp-24-13285-2024-supplement.

Author contributions. Conceptualization: CV, RKC, CN, TSK; methodology, formal analysis: RKC, CN, TSK; software, visualization: CN; data curation and investigation: CN, TSK, GA; writing – original draft: CN; writing – review and editing: TSK, RKC, CV, HCP, GA; supervision: RKC, CV, HCP.

Competing interests. The contact author has declared that none of the authors has any competing interests.

Disclaimer. The views expressed in this document are solely those of authors and do not necessarily reflect those of the Indian Ministry of Environment, Forest and Climate Change. The ministry does not endorse any products or commercial services mentioned in this publication.

Publisher's note: Copernicus Publications remains neutral with regard to jurisdictional claims made in the text, published maps, institutional affiliations, or any other geographical representation in this paper. While Copernicus Publications makes every effort to include appropriate place names, the final responsibility lies with the authors.

Acknowledgements. The authors thank the United States–India Educational Foundation and the IIT Bombay-WashU Aerosol Research and Education Initiative for financial support to conduct a part of this work at Washington University in St. Louis. This work was supported by the Indian Ministry of Environment, Forest and Climate Change under the NCAP-COALESCE project.

Financial support. This research has been supported by the United States–India Educational Foundation (Fulbright-Kalam Climate Fellowship, award no. 2913/FNDR/2023-2024, to Chimurkar Navinya); IIT Bombay-WashU Aerosol Research and Education Initiative; and the Indian Ministry of Environment, Forest and Climate Change under the NCAP-COALESCE project (grant no. 14/10/2014-CC(Vol.II)).

Review statement. This paper was edited by Duncan Watson-Parris and reviewed by two anonymous referees.

References

Arola, A., Schuster, G. L., Pitkänen, M. R. A., Dubovik, O., Kokkola, H., Lindfors, A. V., Mielonen, T., Raatikainen, T., Romakkaniemi, S., Tripathi, S. N., and Lihavainen, H.: Direct radiative effect by brown carbon over the Indo-Gangetic Plain, Atmos. Chem. Phys., 15, 12731–12740, https://doi.org/10.5194/acp-15-12731-2015, 2015.

Azhar, R., Zeeshan, M., and Fatima, K.: Crop residue open field burning in Pakistan; multi-year high spatial resolution emission inventory for 2000–2014, Atmos. Environ., 208, 20–33, https://doi.org/10.1016/J.ATMOSENV.2019.03.031, 2019.

Bhowmik, H. S., Tripathi, S. N., Shukla, A. K., Lalchandani, V., Murari, V., Devaprasad, M., Shivam, A., Bhushan, R., Prévôt, A. S. H., and Rastogi, N.: Contribution of fossil and biomass-derived secondary organic carbon to winter water-soluble organic aerosols in Delhi, India, Sci. Total Environ., 912, 168655, https://doi.org/10.1016/J.SCITOTENV.2023.168655, 2024.

Bikkina, P., Bikkina, S., Kawamura, K., Sudheer, A. K., Mahesh, G., and Kumar, S. K.: Evidence for brown carbon absorption over the Bay of Bengal during the southwest monsoon season: A possible oceanic source, Environ. Sci.-Proc. Imp., 22, 1743–1758, https://doi.org/10.1039/d0em00111b, 2020.

Bikkina, S. and Sarin, M.: Brown carbon in the continental outflow to the North Indian Ocean, Environ. Sci.-Proc. Imp., 21, 970–987, https://doi.org/10.1039/c9em00089e, 2019.

Bond, T. C. and Bergstrom, R. W.: Light absorption by carbonaceous particles: An investigative review, Aerosol Sci. Technol., 40, 27–67, https://doi.org/10.1080/02786820500421521, 2006.

Bond, T. C., Doherty, S. J., Fahey, D. W., Forster, P. M., Berntsen, T., Deangelo, B. J., Flanner, M. G., Ghan, S., Kärcher, B., Koch, D., Kinne, S., Kondo, Y., Quinn, P. K., Sarofim, M. C., Schultz, M. G., Schulz, M., Venkataraman, C., Zhang, H., Zhang, S., Bellouin, N., Guttikunda, S. K., Hopke, P. K., Jacobson, M. Z., Kaiser, J. W., Klimont, Z., Lohmann, U., Schwarz, J. P., Shindell, D., Storelvmo, T., Warren, S. G., and Zender, C. S.: Bounding the role of black carbon in the climate system: A scientific assessment, J. Geophys. Res.-Atmos., 118, 5380–5552, https://doi.org/10.1002/JGRD.50171, 2013.

Bonjour, S., Adair-Rohani, H., Wolf, J., Bruce, N. G., Mehta, S., Prüss-Ustün, A., Lahiff, M., Rehfuess, E. A., Mishra, V., and Smith, K. R.: Solid fuel use for household cooking: Country and regional estimates for 1980–2010, Environ. Health Persp., 121, 784–790, https://doi.org/10.1289/EHP.1205987, 2013.

Boreddy, S. K. R., Hegde, P., Aswini, A. R., and Aryasree, S.: Chemical Characteristics, Size Distributions, Molecular Composition, and Brown Carbon in South Asian Outflow to the Indian Ocean, Earth Space Sci., 8, 1–32, https://doi.org/10.1029/2020EA001615, 2021.

Brown, H., Liu, X., Feng, Y., Jiang, Y., Wu, M., Lu, Z., Wu, C., Murphy, S., and Pokhrel, R.: Radiative effect and climate impacts of brown carbon with the Community Atmosphere Model (CAM5), Atmos. Chem. Phys., 18, 17745–17768, https://doi.org/10.5194/acp-18-17745-2018, 2018.

Chakrabarty, R. K., Moosmüller, H., Chen, L.-W. A., Lewis, K., Arnott, W. P., Mazzoleni, C., Dubey, M. K., Wold, C. E., Hao, W. M., and Kreidenweis, S. M.: Brown carbon in tar balls from smoldering biomass combustion, Atmos. Chem. Phys., 10, 6363–6370, https://doi.org/10.5194/acp-10-6363-2010, 2010.

Chakrabarty, R. K., Shetty, N. J., Thind, A. S., Beeler, P., Sumlin, B. J., Zhang, C., Liu, P., Idrobo, J. C., Adachi, K., Wagner, N. L., Schwarz, J. P., Ahern, A., Sedlacek, A. J., Lambe, A., Daube, C., Lyu, M., Liu, C., Herndon, S., Onasch, T. B., and Mishra, R.: Shortwave absorption by wildfire smoke dominated by dark brown carbon, Nat. Geosci., 16, 683–688, https://doi.org/10.1038/s41561-023-01237-9, 2023.

Chelluboyina, G. S., Kapoor, T. S., and Chakrabarty, R. K.: Dark brown carbon from wildfires: a potent snow radiative forcing agent?, npj Clim. Atmos. Sci., 7, 200, https://doi.org/10.1038/s41612-024-00738-7, 2024.

Chen, L. W. A., Chow, J. C., Wang, X., Cao, J., Mao, J., and Watson, J. G.: Brownness of Organic Aerosol over the United States: Evidence for Seasonal Biomass Burning and Photobleaching Effects, Environ. Sci. Technol., 55, 8561–8572, https://doi.org/10.1021/ACS.EST.0C08706, 2021.

Chen, Y. and Bond, T. C.: Light absorption by organic carbon from wood combustion, Atmos. Chem. Phys., 10, 1773–1787, https://doi.org/10.5194/acp-10-1773-2010, 2010.

Cheng, Z., Atwi, K., Hajj, O. El, Ijeli, I., Fischer, D. Al, Smith, G., and Saleh, R.: Discrepancies between brown carbon light-absorption properties retrieved from online and offline measurements, Aerosol Sci. Technol., 55, 92–103, https://doi.org/10.1080/02786826.2020.1820940, 2021.

Choudhary, V., Rajput, P., Rajeev, P., and Gupta, T.: Synergistic effect in absorption properties of brown carbon and elemental carbon over IGP during weak south-west monsoon, Aerosol Sci. Eng., 1, 138–149, https://doi.org/10.1007/s41810-017-0013-1, 2017.

Choudhary, V., Rajput, P., Singh, D. K., Singh, A. K., and Gupta, T.: Light absorption characteristics of brown carbon during foggy and non-foggy episodes over the Indo–Gangetic Plain, Atmos. Pollut. Res., 9, 494–501, https://doi.org/10.1016/j.apr.2017.11.012, 2018.

Choudhary, V., Singh, G. K., Gupta, T., and Paul, D.: Absorption and radiative characteristics of brown carbon aerosols during crop residue burning in the source region of Indo–Gangetic Plain, Atmos. Res., 249, 105285, https://doi.org/10.1016/j.atmosres.2020.105285, 2021.

Choudhary, V., Gupta, T., and Zhao, R.: Evolution of Brown Carbon Aerosols during Atmospheric Long-Range Transport in the South Asian Outflow and Himalayan Cryosphere, ACS Earth Sp. Chem., 6, 2335–2347, https://doi.org/10.1021/acsearthspacechem.2c00047, 2022.

Chow, J. C., Watson, J. G., Chen, L. W. A., Chang, M. C. O., Robinson, N. F., Trimble, D., and Kohl, S.: The IMPROVE_A

Temperature Protocol for Thermal/Optical Carbon Analysis: Maintaining Consistency with a Long-Term Database, J. Air Waste Manage., 57, 1014–1023, https://doi.org/10.3155/1047-3289.57.9.1014, 2007.

Chow, J. C., Lowenthal, D. H., Chen, L. W. A., Wang, X., and Watson, J. G.: Mass reconstruction methods for $PM_{2.5}$: a review, Air Qual. Atmos. Hlth., 8, 243–263, https://doi.org/10.1007/s11869-015-0338-3, 2015.

Corbin, J. C., Czech, H., Massabò, D., de Mongeot, F. B., Jakobi, G., Liu, F., Lobo, P., Mennucci, C., Mensah, A. A., Orasche, J., Pieber, S. M., Prévôt, A. S. H., Stengel, B., Tay, L. L., Zanatta, M., Zimmermann, R., El Haddad, I., and Gysel, M.: Infrared-absorbing carbonaceous tar can dominate light absorption by marine-engine exhaust, npj Clim. Atmos. Sci., 21, 1–10, https://doi.org/10.1038/s41612-019-0069-5, 2019.

Crippa, M., Guizzardi, D., Muntean, M., Schaaf, E., Dentener, F., van Aardenne, J. A., Monni, S., Doering, U., Olivier, J. G. J., Pagliari, V., and Janssens-Maenhout, G.: Gridded emissions of air pollutants for the period 1970–2012 within EDGAR v4.3.2, Earth Syst. Sci. Data, 10, 1987–2013, https://doi.org/10.5194/essd-10-1987-2018, 2018.

Dasari, S., Andersson, A., Bikkina, S., Holmstrand, H., Budhavant, K., Satheesh, S., Asmi, E., Kesti, J., Backman, J., Salam, A., Bisht, D. S., Tiwari, S., Hameed, Z., and Gustafsson, Ö.: Photochemical degradation affects the light absorption of water-soluble brown carbon in the South Asian outflow, Sci. Adv., 5, 1–11, https://doi.org/10.1126/sciadv.aau8066, 2019.

Debbarma, S., Raparthi, N., Venkataraman, C., and Phuleria, H. C.: Characterization and apportionment of carbonaceous aerosol emission factors from light-duty and heavy-duty vehicle fleets in Maharashtra, India, Environ. Pollut., 345, 123479, https://doi.org/10.1016/J.ENVPOL.2024.123479, 2024.

Devaprasad, M., Rastogi, N., Satish, R., Patel, A., Dabhi, A., Shivam, A., Bhushan, R., and Meena, R.: Dual carbon isotope-based brown carbon aerosol characteristics at a high-altitude site in the northeastern Himalayas: Role of biomass burning, Sci. Total Environ., 912, 169451, https://doi.org/10.1016/J.SCITOTENV.2023.169451, 2024.

Dey, S., Mukherjee, A., Polana, A. J., Rana, A., Mao, J., Jia, S., Yadav, A. K., Khillare, P. S., and Sarkar, S.: Brown carbon aerosols in the Indo–Gangetic Plain outflow: Insights from excitation emission matrix (EEM) fluorescence spectroscopy, Environ. Sci.-Proc. Imp., 23, 745–755, https://doi.org/10.1039/d1em00050k, 2021.

Dey, S., Ghosh, P., Rawat, P., Choudhary, N., Rai, A., Meena, R., Mandal, T. K., Mao, J., Jia, S., Rastogi, N., Sharma, S. K., and Sarkar, S.: Optical source apportionment of aqueous brown carbon (BrC) on a daytime and nighttime basis in the eastern Indo–Gangetic Plain (IGP) and insights from ^{13}C and ^{15}N isotopic signatures, Sci. Total Environ., 894, 164872, https://doi.org/10.1016/j.scitotenv.2023.164872, 2023.

DRI Manual: DRI Model 2015 Multiwavelength Thermal/Optical Carbon Analyzer Installation, Operation, and Service Manual, Aerosol Magee Scientific, https://www.aerosolmageesci.com/products/dri-model-2015-series-2/ (last access: 14 April 2024), 2015.

Feng, Y., Ramanathan, V., and Kotamarthi, V. R.: Brown carbon: a significant atmospheric absorber of solar radiation?, Atmos. Chem. Phys., 13, 8607–8621, https://doi.org/10.5194/acp-13-8607-2013, 2013.

Gliß, J., Mortier, A., Schulz, M., Andrews, E., Balkanski, Y., Bauer, S. E., Benedictow, A. M. K., Bian, H., Checa-Garcia, R., Chin, M., Ginoux, P., Griesfeller, J. J., Heckel, A., Kipling, Z., Kirkevåg, A., Kokkola, H., Laj, P., Le Sager, P., Lund, M. T., Lund Myhre, C., Matsui, H., Myhre, G., Neubauer, D., van Noije, T., North, P., Olivié, D. J. L., Rémy, S., Sogacheva, L., Takemura, T., Tsigaridis, K., and Tsyro, S. G.: AeroCom phase III multi-model evaluation of the aerosol life cycle and optical properties using ground- and space-based remote sensing as well as surface in situ observations, Atmos. Chem. Phys., 21, 87–128, https://doi.org/10.5194/acp-21-87-2021, 2021.

Gyawali, M., Arnott, W. P., Zaveri, R. A., Song, C., Pekour, M., Flowers, B., Dubey, M. K., Setyan, A., Zhang, Q., Harworth, J. W., Radney, J. G., Atkinson, D. B., China, S., Mazzoleni, C., Gorkowski, K., Subramanian, R., Jobson, B. T., and Moosmüller, H.: Evolution of multispectral aerosol optical properties in a biogenically-influenced urban environment during the CARES campaign, Atmos. Chem. Phys. Discuss., 13, 7113–7150, https://doi.org/10.5194/acpd-13-7113-2013, 2013.

Habib, G., Kumari, J., Khan, M., Zaidi, K., Yogesh, A., Nagendra, S. M. S., Navinya, C., Phuleria, H., Bombay, I., Arya, R., Mandal, T., Delhi, N., Muthalagu, A., Qureshi, A., Bhat, R., and Jehangir, A.: Estimating shifts in fuel stacking among solid biomass fuels and liquified petroleum gas in rural households: A pan-India analysis, Research Square [preprint], https://doi.org/10.21203/rs.3.rs-2674609/v1, 2023.

Hecobian, A., Zhang, X., Zheng, M., Frank, N., Edgerton, E. S., and Weber, R. J.: Water-Soluble Organic Aerosol material and the light-absorption characteristics of aqueous extracts measured over the Southeastern United States, Atmos. Chem. Phys., 10, 5965–5977, https://doi.org/10.5194/acp-10-5965-2010, 2010.

Islam, M. M., Neyestani, S. E., Saleh, R., and Grieshop, A. P.: Quantifying brown carbon light absorption in real-world biofuel combustion emissions, Aerosol Sci. Technol., 56, 502–516, https://doi.org/10.1080/02786826.2022.2051425, 2022.

Jennings, S. G., Pinnick, R. G., and Gillespie, J. B.: Relation between absorption coefficient and imaginary index of atmospheric aerosol constituents, Appl. Optics, 18, 1368, https://doi.org/10.1364/ao.18.001368, 1979.

Kapoor, T. S., Venkataraman, C., Sarkar, C., Phuleria, H. C., Chatterjee, A., Habib, G., and Apte, J. S.: Estimation of real-time brown carbon absorption: An observationally constrained Mie theory-based optimization method, J. Aerosol Sci., 106047, https://doi.org/10.1016/J.JAEROSCI.2022.106047, 2022.

Kapoor, T. S., Phuleria, H. C., Sumlin, B., Shetty, N., Anurag, G., Bansal, M., Duhan, S. S., Khan, M. S., Laura, J. S., Manwani, P., Chakrabarty, R. K., and Venkataraman, C.: Optical Properties and Refractive Index of Wintertime Aerosol at a Highly Polluted North-Indian Site, J. Geophys. Res.-Atmos., 128, 1–14, https://doi.org/10.1029/2022JD038272, 2023a.

Kapoor, T. S., Navinya, C., Anurag, G., Lokhande, P., Rathi, S., Goel, A., Sharma, R., Arya, R., Mandal, T. K., Jithin, K. P., Nagendra, S., Imran, M., Kumari, J., Muthalagu, A., Qureshi, A., Najar, T. A., Jehangir, A., Haswani, D., Raman, R. S., Rabha, S., Saikia, B., Lian, Y., Pandithurai, G., Chaudhary, P., Sinha, B., Dhandapani, A., Iqbal, J., Mukherjee, S., Chatterjee, A., Venkataraman, C., and Phuleria, H. C.: Reassessing the

availability of crop residue as a bioenergy resource in India: A field-survey based study, J. Environ. Manage., 341, 118055, https://doi.org/10.1016/j.jenvman.2023.118055, 2023b.

Kirchstetter, T. W., Novakov, T., and Hobbs, P. V.: Evidence that the spectral dependence of light absorption by aerosols is affected by organic carbon, J. Geophys. Res.-Atmos., 109, 1–12, https://doi.org/10.1029/2004JD004999, 2004.

Kirillova, E. N., Marinoni, A., Bonasoni, P., Vuillermoz, E., Facchini, M. C., Fuzzi, S., and Decesari, S.: Light absorption properties of brown carbon in the high Himalayas, J. Geophys. Res., 121, 9621–9639, https://doi.org/10.1002/2016JD025030, 2016.

Kroll, J. H. and Seinfeld, J. H.: Chemistry of secondary organic aerosol: Formation and evolution of low-volatility organics in the atmosphere, Atmos. Environ., 42, 3593–3624, https://doi.org/10.1016/J.ATMOSENV.2008.01.003, 2008.

Kroll, J. H., Chan, A. W. H., Ng, N. L., Flagan, R. C., and Seinfeld, J. H.: Reactions of semivolatile organics and their effects on secondary organic aerosol formation, Environ. Sci. Technol., 41, 3545–3550, https://doi.org/10.1021/ES062059X, 2007.

Kumar, V., Malyan, V., Sahu, M., Biswal, B., Pawar, M., and Dev, I.: Spatiotemporal analysis of fine particulate matter for India (1980–2021) from MERRA-2 using ensemble machine learning, Atmos. Pollut. Res., 14, 101834, https://doi.org/10.1016/J.APR.2023.101834, 2023.

Kumari, J., Khan, M. S., Bansal, M., Kapoor, T. S., and Habib, G.: Design, evaluation, and performance of portable sampling trains for monitoring and characterization of aerosols from mobile and stationary combustion sources, Aerosol Sci. Technol., 58, 1333–1346, https://doi.org/10.1080/02786826.2024.2412992, 2024.

Kurokawa, J. and Ohara, T.: Long-term historical trends in air pollutant emissions in Asia: Regional Emission inventory in ASia (REAS) version 3, Atmos. Chem. Phys., 20, 12761–12793, https://doi.org/10.5194/acp-20-12761-2020, 2020.

Kuwata, M., Zorn, S. R., and Martin, S. T.: Using elemental ratios to predict the density of organic material composed of carbon, hydrogen, and oxygen, Environ. Sci. Technol., 46, 787–794, https://doi.org/10.1021/ES202525Q, 2012.

Lack, D. A., Langridge, J. M., Bahreini, R., Cappa, C. D., Middlebrook, A. M., and Schwarz, J. P.: Brown carbon and internal mixing in biomass burning particles, P. Natl. Acad. Sci. USA, 109, 14802–14807, https://doi.org/10.1073/PNAS.1206575109, 2012.

Lee, J., Kim, J., Song, C. H., Kim, S. B., Chun, Y., Sohn, B. J., and Holben, B. N.: Characteristics of aerosol types from AERONET sunphotometer measurements, Atmos. Environ., 44, 3110–3117, https://doi.org/10.1016/J.ATMOSENV.2010.05.035, 2010.

Lin, G., Penner, J. E., Flanner, M. G., Sillman, S., Xu, L., and Zhou, C.: Radiative forcing of organic aerosol in the atmosphere and on snow: Effects of SOA and brown carbon, J. Geophys. Res., 119, 7453–7476, https://doi.org/10.1002/2013JD021186, 2014.

Liu, C., Chung, C. E., Yin, Y., and Schnaiter, M.: The absorption Ångström exponent of black carbon: from numerical aspects, Atmos. Chem. Phys., 18, 6259–6273, https://doi.org/10.5194/acp-18-6259-2018, 2018.

Liu, J., Bergin, M., Guo, H., King, L., Kotra, N., Edgerton, E., and Weber, R. J.: Size-resolved measurements of brown carbon in water and methanol extracts and estimates of their contribution to ambient fine-particle light absorption, Atmos. Chem. Phys., 13, 12389–12404, https://doi.org/10.5194/acp-13-12389-2013, 2013.

Lu, Z., Streets, D. G., Winijkul, E., Yan, F., Chen, Y., Bond, T. C., Feng, Y., Dubey, M. K., Liu, S., Pinto, J. P., and Carmichael, G. R.: Light absorption properties and radiative effects of primary organic aerosol emissions, Environ. Sci. Technol., 49, 4868–4877, https://doi.org/10.1021/ACS.EST.5B00211, 2015.

Luo, B., Kuang, Y., Huang, S., Song, Q., Hu, W., Li, W., Peng, Y., Chen, D., Yue, D., Yuan, B., and Shao, M.: Parameterizations of size distribution and refractive index of biomass burning organic aerosol with black carbon content, Atmos. Chem. Phys., 22, 12401–12415, https://doi.org/10.5194/acp-22-12401-2022, 2022.

Ma, J., Li, X., Gu, P., Dallmann, T. R., Presto, A. A., and Donahue, N. M.: Estimating ambient particulate organic carbon concentrations and partitioning using thermal optical measurements and the volatility basis set, Aerosol Sci. Technol., 50, 638–651, https://doi.org/10.1080/02786826.2016.1158778, 2016.

McDuffie, E. E., Smith, S. J., O'Rourke, P., Tibrewal, K., Venkataraman, C., Marais, E. A., Zheng, B., Crippa, M., Brauer, M., and Martin, R. V.: A global anthropogenic emission inventory of atmospheric pollutants from sector- and fuel-specific sources (1970–2017): an application of the Community Emissions Data System (CEDS), Earth Syst. Sci. Data, 12, 3413–3442, https://doi.org/10.5194/essd-12-3413-2020, 2020.

Mcmeeking, G. R.: Dissertation the optical, chemical, and physical properties of aerosols and gases emitted by the laboratory combustion of wildland fuels, ProQuest Dissertations And Theses, Thesis (PhD), Colorado State University, 298 pp., ISBN 9781109013443, 2008.

Mukherjee, A., Dey, S., Rana, A., Jia, S., Banerjee, S., and Sarkar, S.: Sources and atmospheric processing of brown carbon and HULIS in the Indo–Gangetic Plain: Insights from compositional analysis, Environ. Pollut., 267, 115440, https://doi.org/10.1016/j.envpol.2020.115440, 2020.

Navinya, C., Kapoor, T. S., Gupta, A. K., Lokhande, P., Sharma, R., SV, L. P., SM, S. N., Kumari, J., Habib, G., Arya, R., Mandal, T. K., Muthalagu, A., Qureshi, A., Najar, T. A., Jehangir, A., Jain, S., Goel, A., Rabha, S., Saikia, B., Chaudhary, P., Sinha, B., Haswani, D., Raman, R. S., Dhandapani, A., Iqbal, J., Mukherjee, S., Chatterjee, A., Lian, Y., Pandithurai, G., Venkataraman, C., and Phuleria, H. C.: Heating and lighting: Understanding overlooked energy-consumption activities in the Indian residential sector, Environ. Res. Commun., 5, 045004, https://doi.org/10.1088/2515-7620/ACCA6F, 2023.

Navinya, C. D., Vinoj, V., and Pandey, S. K.: Evaluation of $PM_{2.5}$ surface concentrations simulated by NASA's MERRA version 2 aerosol reanalysis over india and its relation to the air quality index, Aerosol Air Qual. Res., 20, 1329–1339, https://doi.org/10.4209/aaqr.2019.12.0615, 2020.

Neyestani, S. E. and Saleh, R.: Observationally constrained representation of brown carbon emissions from wildfires in a chemical transport model, Environ. Sci. Atmos., 2, 192–201, https://doi.org/10.1039/D1EA00059D, 2022.

Ohara, T., Akimoto, H., Kurokawa, J., Horii, N., Yamaji, K., Yan, X., and Hayasaka, T.: An Asian emission inventory of anthropogenic emission sources for the period 1980–2020, Atmos. Chem. Phys., 7, 4419–4444, https://doi.org/10.5194/acp-7-4419-2007, 2007.

Pandey, A., Sadavarte, P., Rao, A. B., and Venkataraman, C.: Trends in multi-pollutant emissions from a technology-linked inventory for India: II. Residential, agricultural and informal industry sectors, Atmos. Environ., 99, 341–352, https://doi.org/10.1016/j.atmosenv.2014.09.080, 2014.

Pandey, A., Hsu, A., Tiwari, S., Pervez, S., and Chakrabarty, R. K.: Light Absorption by Organic Aerosol Emissions Rivals That of Black Carbon from Residential Biomass Fuels in South Asia, Environ. Sci. Tech. Let., 7, 266–272, https://doi.org/10.1021/acs.estlett.0c00058, 2020.

Park, R. J., Kim, M. J., Jeong, J. I., Youn, D., and Kim, S.: A contribution of brown carbon aerosol to the aerosol light absorption and its radiative forcing in East Asia, Atmos. Environ., 44, 1414–1421, https://doi.org/10.1016/J.ATMOSENV.2010.01.042, 2010.

Provençal, S., Buchard, V., da Silva, A. M., Leduc, R., Barrette, N., Elhacham, E., and Wang, S. H.: Evaluation of $PM_{2.5}$ surface concentrations simulated by version 1 of NASA's MERRA aerosol reanalysis over Israel and Taiwan, Aerosol Air Qual. Res., 17, 253–261, https://doi.org/10.4209/aaqr.2016.04.0145, 2017.

Rajeev, P., Choudhary, V., Chakraborty, A., and Kumar, G.: Light absorption potential of water-soluble organic aerosols in the two polluted urban locations in the central Indo–Gangetic Plain?, Environ. Pollut., 314, 120228, https://doi.org/10.1016/j.envpol.2022.120228, 2022.

Rana, A., Dey, S., Rawat, P., Mukherjee, A., Mao, J., Jia, S., Khillare, P. S., Yadav, A. K., and Sarkar, S.: Optical properties of aerosol brown carbon (BrC) in the eastern Indo–Gangetic Plain, Sci. Total Environ., 716, 137102, https://doi.org/10.1016/j.scitotenv.2020.137102, 2020.

Rastogi, N., Satish, R., Singh, A., Kumar, V., Thamban, N., Lalchandani, V., Shukla, A., Vats, P., Tripathi, S. N., Ganguly, D., Slowik, J., and Prevot, A. S. H.: Diurnal variability in the spectral characteristics and sources of water-soluble brown carbon aerosols over Delhi, Sci. Total Environ., 794, 148589, https://doi.org/10.1016/j.scitotenv.2021.148589, 2021.

Rathod, T., Sahu, S. K., Tiwari, M., Yousaf, A., Bhangare, R. C., and Pandit, G. G.: Light absorbing properties of brown carbon generated from pyrolytic combustion of household biofuels, Aerosol Air Qual. Res., 17, 108–116, https://doi.org/10.4209/aaqr.2015.11.0639, 2017.

Roden, C. A., Bond, T. C., Conway, S., and Osorto Pinel, A. B.: Emission factors and real-time optical properties of particles emitted from traditional wood burning cookstoves, Environ. Sci. Technol., 40, 6750–6757, https://doi.org/10.1021/es052080i, 2006.

Romonosky, D. E., Ali, N. N., Saiduddin, M. N., Wu, M., Lee, H. J. J., Aiona, P. K., and Nizkorodov, S. A.: Effective absorption cross sections and photolysis rates of anthropogenic and biogenic secondary organic aerosols, Atmos. Environ., 130, 172–179, https://doi.org/10.1016/J.ATMOSENV.2015.10.019, 2016.

Roy, S., Lam, Y. F., Hoque, M. M., and Chopra, S. S.: Review of Decadal Changes in ASEAN Emissions Based on Regional and Global Emission Inventory Datasets, Aerosol Air Qual. Res., 23, 220103, https://doi.org/10.4209/AAQR.220103, 2023.

Sadavarte, P., Rupakheti, M., Bhave, P., Shakya, K., and Lawrence, M.: Nepal emission inventory – Part I: Technologies and combustion sources (NEEMI-Tech) for 2001–2016, Atmos. Chem. Phys., 19, 12953–12973, https://doi.org/10.5194/acp-19-12953-2019, 2019.

Saleh, R.: From Measurements to Models: Toward Accurate Representation of Brown Carbon in Climate Calculations, Curr. Pollut. Reports, 6, 90–104, https://doi.org/10.1007/s40726-020-00139-3, 2020.

Saleh, R., Robinson, E. S., Tkacik, D. S., Ahern, A. T., Liu, S., Aiken, A. C., Sullivan, R. C., Presto, A. A., Dubey, M. K., Yokelson, R. J., Donahue, N. M., and Robinson, A. L.: Brownness of organics in aerosols from biomass burning linked to their black carbon content, Nat. Geosci., 7, 647–650, https://doi.org/10.1038/NGEO2220, 2014.

Saleh, R., Cheng, Z., and Atwi, K.: The Brown-Black Continuum of Light-Absorbing Combustion Aerosols, Environ. Sci. Tech. Let., 5, 508–513, https://doi.org/10.1021/acs.estlett.8b00305, 2018.

Sand, M., Samset, B. H., Myhre, G., Gliß, J., Bauer, S. E., Bian, H., Chin, M., Checa-Garcia, R., Ginoux, P., Kipling, Z., Kirkevåg, A., Kokkola, H., Le Sager, P., Lund, M. T., Matsui, H., van Noije, T., Olivié, D. J. L., Remy, S., Schulz, M., Stier, P., Stjern, C. W., Takemura, T., Tsigaridis, K., Tsyro, S. G., and Watson-Parris, D.: Aerosol absorption in global models from AeroCom phase III, Atmos. Chem. Phys., 21, 15929–15947, https://doi.org/10.5194/acp-21-15929-2021, 2021.

Sarkar, C., Venkataraman, C., Yadav, S., Phuleria, H. C., and Chatterjee, A.: Origin and properties of soluble brown carbon in freshly emitted and aged ambient aerosols over an urban site in India, Environ. Pollut., 254, 113077, https://doi.org/10.1016/j.envpol.2019.113077, 2019.

Satish, R. and Rastogi, N.: On the Use of Brown Carbon Spectra as a Tool to Understand Their Broader Composition and Characteristics: A Case Study from Crop-residue Burning Samples, ACS Omega, 4, 1814–1853, https://doi.org/10.1021/acsomega.8b02637, 2019.

Satish, R., Rastogi, N., Singh, A., and Singh, D.: Change in characteristics of water-soluble and water-insoluble brown carbon aerosols during a large-scale biomass burning, Environ. Sci. Pollut. R., 27, 33339–33350, https://doi.org/10.1007/s11356-020-09388-7, 2020.

Shamjad, P. M., Tripathi, S. N., Thamban, N. M., and Vreeland, H.: Refractive index and absorption attribution of highly absorbing brown carbon aerosols from an urban Indian city-Kanpur, Sci. Rep., 6, 37735, https://doi.org/10.1038/SREP37735, 2016.

Shamjad, P. M., Satish, R. V., Thamban, N. M., Rastogi, N., and Tripathi, S. N.: Absorbing Refractive Index and Direct Radiative Forcing of Atmospheric Brown Carbon over Gangetic Plain, ACS Earth Sp. Chem., 2, 31–37, https://doi.org/10.1021/acsearthspacechem.7b00074, 2018.

Shetty, N., Liu, P., Liang, Y., Sumlin, B., Daube, C., Herndon, S., Goldstein, A. H., and Chakrabarty, R. K.: Brown carbon absorptivity in fresh wildfire smoke: associations with volatility and chemical compound groups, Environ. Sci. Atmos., 3, 1262–1271, https://doi.org/10.1039/d3ea00067b, 2023.

Soleimanian, E., Mousavi, A., Taghvaee, S., Sowlat, M. H., Hasheminassab, S., Polidori, A., and Sioutas, C.: Spatial trends and sources of $PM_{2.5}$ organic carbon volatility fractions (OC_X) across the Los Angeles Basin, Atmos. Environ., 209, 201–211, https://doi.org/10.1016/J.ATMOSENV.2019.04.027, 2019.

Srinivas, B. and Sarin, M. M.: Light absorbing organic aerosols (brown carbon) over the tropical Indian Ocean: Impact of

biomass burning emissions, Environ. Res. Lett., 8, 044042, https://doi.org/10.1088/1748-9326/8/4/044042, 2013.

Srinivas, B. and Sarin, M. M.: Brown carbon in atmospheric outflow from the Indo–Gangetic Plain: Mass absorption efficiency and temporal variability, Atmos. Environ., 89, 835–843, https://doi.org/10.1016/j.atmosenv.2014.03.030, 2014.

Sumlin, B. J., Pandey, A., Walker, M. J., Pattison, R. S., Williams, B. J., and Chakrabarty, R. K.: Atmospheric Photooxidation Diminishes Light Absorption by Primary Brown Carbon Aerosol from Biomass Burning, Environ. Sci. Tech. Let., 4, 540–545, https://doi.org/10.1021/ACS.ESTLETT.7B00393, 2017.

Szopa, S., Naik, V., Adhikary, B., Artaxo, P., Berntsen, T., Collins, W. D., Fuzzi, S., Gallardo, L., Kiendler Scharr, A., Klimont, Z., Liao, H., Unger, N., and Zanis, P.: Short-Lived Climate Forcers, in: Climate Change 2021 – The Physical Science Basis: Working Group I Contribution to the Sixth Assessment Report of the Intergovernmental Panel on Climate Change, Cambridge University Press, https://doi.org/10.1017/9781009157896.008, 817–922, 2021.

Tibrewal, K., Venkataraman, C., Phuleria, H., Joshi, V., Maithel, S., Damle, A., Gupta, A., Lokhande, P., Rabha, S., Saikia, B. K., Roy, S., Habib, G., Rathi, S., Goel, A., Ahlawat, S., Mandal, T. K., Azharuddin Hashmi, M., Qureshi, A., Dhandapani, A., Iqbal, J., Devaliya, S., Raman, R. S., Lian, Y., Pandithurai, G., Kuppili, S. K., Shiva Nagendra, M., Mukherjee, S., Chatterjee, A., Najar, T. A., Jehangir, A., Singh, J., and Sinha, B.: Reconciliation of energy use disparities in brick production in India, Nat. Sustain., 6, 1248–1257, https://doi.org/10.1038/s41893-023-01165-x, 2023.

Tibrewal, K., Venkataraman, C., Habib, G., Phuleria, H., Gupta, A., Gupta, G., Kumari, J., Chimurkar, N. D., Khan, S., and Singh Kapoor, T.: Country level anthropogenic emissions of GHGs and air pollutants over India for 2019 from Speciated Multipollutant Generator (SMoG)-India COALESCE emissions inventory (v0_2024_Jan_31), Zenodo [data set], https://doi.org/10.5281/zenodo.10602217, 2024.

Tock, J. Y., Lai, C. L., Lee, K. T., Tan, K. T., and Bhatia, S.: Banana biomass as potential renewable energy resource: A Malaysian case study, Renew. Sust. Energ. Rev., 14, 798–805, https://doi.org/10.1016/J.RSER.2009.10.010, 2010.

Tohidi, R., Altuwayjiri, A., and Sioutas, C.: Investigation of organic carbon profiles and sources of coarse PM in Los Angeles, Environ. Pollut., 314, 120264, https://doi.org/10.1016/J.ENVPOL.2022.120264, 2022.

Turpin, B. J. and Lim, H.: Species Contributions to $PM_{2.5}$ Mass Concentrations: Revisiting Common Assumptions for Estimating Organic Mass, Aerosol Sci. Tech., 35, 602–610, https://doi.org/10.1080/02786820119445, 2001.

Venkataraman, C., Bhushan, M., Dey, S., Ganguly, D., Gupta, T., Habib, G., Kesarkar, A., Phuleria, H., and Raman, R. S.: Indian Network Project on Carbonaceous Aerosol Emissions, Source Apportionment and Climate Impacts (COALESCE), B. Am. Meteorol. Soc., 101, E1052–E1068, https://doi.org/10.1175/BAMS-D-19-0030.1, 2020.

Vodička, P., Schwarz, J., Cusack, M., and Ždímal, V.: Detailed comparison of OC/EC aerosol at an urban and a rural Czech background site during summer and winter, Sci. Total Environ., 518–519, 424–433, https://doi.org/10.1016/J.SCITOTENV.2015.03.029, 2015.

Wang, J., Nie, W., Cheng, Y., Shen, Y., Chi, X., Wang, J., Huang, X., Xie, Y., Sun, P., Xu, Z., Qi, X., Su, H., and Ding, A.: Light absorption of brown carbon in eastern China based on 3-year multi-wavelength aerosol optical property observations and an improved absorption Ångström exponent segregation method, Atmos. Chem. Phys., 18, 9061–9074, https://doi.org/10.5194/acp-18-9061-2018, 2018.

Wang, Y., Hu, M., Li, X., and Xu, N.: Chemical Composition, Sources and Formation Mechanisms of Particulate Brown Carbon in the Atmosphere, Prog. Chem., 32, 627, https://doi.org/10.7536/PC190917, 2020.

Weyant, C., Athalye, V., Ragavan, S., Rajarathnam, U., Lalchandani, D., Maithel, S., Baum, E., and Bond, T. C.: Emissions from South Asian brick production, Environ. Sci. Technol., 48, 6477–6483, https://doi.org/10.1021/ES500186G, 2014.

Yevich, R. and Logan, J. A.: An assessment of biofuel use and burning of agricultural waste in the developing world, Global Biogeochem. Cy., 17, https://doi.org/10.1029/2002GB001952, 2003.

Zhang, A., Wang, Y., Zhang, Y., Weber, R. J., Song, Y., Ke, Z., and Zou, Y.: Modeling the global radiative effect of brown carbon: a potentially larger heating source in the tropical free troposphere than black carbon, Atmos. Chem. Phys., 20, 1901–1920, https://doi.org/10.5194/acp-20-1901-2020, 2020.

Zhu, Y., Wang, Q., Yang, X., Yang, N., and Wang, X.: Modeling investigation of brown carbon aerosol and its light absorption in China, Atmosphere-Basel, 12, 1–12, https://doi.org/10.3390/atmos12070892, 2021.